Molecular dynamics simulation of formation process of single-walled carbon nanotubes by CCVD method

Yasushi Shibuta, Shigeo Maruyama*

Department of Mechanical Engineering, The University of Tokyo

7-3-1 Hongo, Bunkyo-ku, Tokyo 113-8656, Japan

Abstract

Formation process of single-walled carbon nanotubes by the catalytic chemical vapor deposition method is studied by molecular dynamics simulation. We start the calculation with randomly distributed carbon-source molecules and a nickel cluster to investigate the metal-catalyzed growth of a cap-structure of a nanotube. When the catalytic cluster reaches saturation with carbon atoms, hexagonal networks are formed both inside and on the surface of the cluster, leading to their precipitation on the cluster's surface and edges. An appropriate nanotube cap structure is generated when pieces of the hexagonal network structure extending from inside the cluster merges above the metal surface.

*Corresponding Author. Fax: +81-3-5800-6983.

E-mail address: maruyama@photon.t.u-tokyo.ac.jp (S. Maruyama).

1. Introduction

The discovery of single-walled carbon nanotubes (SWNTs) [1] has opened new research and application fields with the carbon material. In addition to initially developed laser-furnace [2] and arc-discharge [3] techniques, catalytic chemical vapor deposition (CCVD) method [4-7] has been contrived for a scalable, large-scale production of SWNTs, with various carbon-source molecules tested such as carbon monoxide [4, 7], methane [5], or ethanol [6]. There are two types of catalysts used in these CVD approaches; one is supported catalysts [4-6] and the other floated (i.e. not supported) catalysts used in e.g. HiPco process [7]. In either way, a proper understanding on the formation mechanism of an SWNT at the catalyst is critically important, besides a theoretical interest, for future control of the diameter and even chirality of SWNTs synthesized through CVD processes.

The formation mechanism of an SWNT has been widely discussed on the basis of results obtained by laser-furnace and arc-discharge experiments. In earlier times, 'scooter model' [2] was proposed as a growth mechanism of SWNTs grown with laser ablation. In this model, a catalytic metal atom sticking on an open edge of a growing SWNT was supposed to prevent the formation of a closure with pentagons by scooting around the edge. In another report, Yudasaka et al. [8] examined several catalytic metal species and their alloys in their laser-furnace experiments and discussed in detail the effect of the choice of catalyst based on their phase diagrams. They suggested a 'metal-particle model', in which droplets of carbon-containing catalytic metal were formed as a consequence of laser ablation and in the subsequent cooling stage the carbon atoms were separated out from the metal nuclei to form SWNTs. Furthermore, Kataura et al. [9] proposed 'fullerene-cap model', where fullerene-like carbon clusters formed during laser-ablation attach to metal particles that served as nuclei for SWNT growth; this model was based on the experimental observation that the growth conditions of fullerene and SWNT were similar and that the diameter distribution of SWNTs was correlated with that of fullerenes.

In contrast, theoretical or numerical contributions to the formation mechanism of carbon nanotubes were limited. Several previous classical molecular dynamics simulations [10, 11] with the Brenner potential [12] or tight-binding molecular dynamics (TBMD) simulation [13] examined the specific points of generation mechanism for pure carbon system. The role of metal catalyst had also been discussed with quantum molecular dynamics (QMD) [14], TBMD simulations [15] and ab initio molecular orbital calculations [16, 17]. These results supported the various mechanisms proposed by such experimental results as 'scooter model' [2, 16], 'diffusing model' [15], and 'root growth model' [14]. Particularly, Gavillet et al. [14] investigated in detail the segregation and diffusion processes separately by QMD simulation, but no sequential simulation for the root growth mechanism because of the computational limit.

Our approach is to use the classical molecular dynamics method for larger systems and longer time-scale simulations. For this purpose, a reliable classical potential function between metal and carbon is necessary. Therefore, we started from constructing the classical potential function between carbon clusters and several atoms (La, Sc and Ni) based on DFT calculations of small metal-carbon binary clusters for simulation of the formation process of endohedral metallofullerene [18]. In our previous studies [19, 20], we simulated 'co-vaporization' by the laser-furnace or arc discharge techniques by starting from an initial state with randomly distributed metal and carbon atoms, and we observed that a metal atom adsorbed to carbon cage clusters prohibited a complete closure of the cage and these partially-open cages worked as a precursor for the formation of imperfect nanotube-like tubular structures. These carbon precursor clusters were confirmed by Fourier transform ion cyclotron resonance (FT-ICR) observations of reactions on laser-vaporized clusters [21]. In this paper, the nucleation and growth processes of SWNTs in the CCVD method is studied by classical molecular dynamics simulations.

2. Simulation techniques

The Brenner potential [12] in its simplified form [22, 23] is used for the carbon-carbon covalent bond. For metal-carbon and metal-metal carbon potential, our previous model [18] is used, which are constructed with the covalent term based on the coordination number of metal atom and the Coulomb term due to the charge transfer from metal to a carbon cluster.

To simplify the simulation, the floated catalyst configuration similar to HiPco process [7] is employed. We assume that a carbon-source molecule such as methane or ethanol decomposes into carbon atoms only on the catalytic metal surface and that the van der Waals potential prohibits clustering of carbon-source molecules. With this assumption, no explicit calculation of hydrogen or oxygen atoms is necessary. The van der Waals term is expressed by the Lennard-Jones (12-6) potential only between intermolecular carbon-carbon atoms with its parameters $\varepsilon = 2.4$ meV and $\sigma = 3.37$ Å. Upon arrival of a carbon-containing molecule to the bare metal surface, it is assumed that complete decomposition and supply of a carbon atom immediately take place. The disproportionation reaction of CO is also regarded as similar to the decomposition of a hydrocarbon. Upon arrival of CO on the metal surface, decomposition of CO and recombination of gas phase CO_2 is assumed to occur. Here, the activation barrier of the chemical reaction process such as decomposition of hydrocarbon or disproportional reaction of CO is simply accounted for by the adjustment of the net flux of carbon supply, though the accurate determination of this reaction process is critically important for the next stages of simulation.

In order to observe the growth process of a longer time scale within the computational limit, the density and the temperature of our system are much higher than the experimental conditions [6]. That is partially compensated by very rapid cooling with a special technique of temperature control [22]. The Berendsen thermostat [24], which is a certain type of the velocity scaling method at regular intervals, is used to control translational, rotational, and vibrational temperatures of the system independently [22]. The relaxation time of the thermostat is set to 0.17 ps. The velocity Verlet method is employed to integrate the classical equation of motion with a time step of 0.5 fs.

3. Results and discussion

We first prepare the initial Ni cluster structures of various sizes by annealing face-centered cubic (fcc) crystal structures for 2 ns at 2000 K. The diameters of the obtained clusters, Ni_{32}, Ni_{108} and Ni_{256}, are roughly 0.8, 1.3 and 1.6 nm, respectively. As the initial condition, a model vapor of 500 carbon-containing molecules and one of the Ni clusters obtained above are randomly allocated in a cubic periodic cell of $(200 \text{ Å})^3$ as in Fig. 1. The initial velocity of molecules is set equivalent to the control temperature T as $\sqrt{3k_B T / m}$. The control temperature is set to 2500 K for subsequent simulations.

3.1. Metal-catalyzed growth process of cap structure

Figure 2 shows the metal-catalyzed growth of the cap structure on Ni_{108} at 2500 K. In the first stage, all carbon atoms attached to the exposed surface are absorbed in the metal cluster. After saturation within about 2 ns, hexagonal carbon networks are formed inside the metal-carbon binary cluster (Fig. 2 (a)). Some of the carbon networks separate from the surface of the particle and in specific cases some cap structures appear, as if the sphere surface of the metal cluster played as a template for cap formation (Fig. 2 (b)). A similar separation process in metal-carbon cluster has also been observed in the previous QMD simulation [14], but the temperature condition and the time scale are different. When separation of the carbon network occurs, the area of bare metal surface decreases but some of the open areas are preserved especially in the crystalline part where additional carbon atoms can still flow. Continuous supply of carbon atoms leads to the formation of annular graphitic protrusion (Fig. 2 (c)). After the cap coalesces into annular graphitic protrusion (Fig. 2 (d)), the larger carbon network covers the surface with a certain curvature (Fig. 2 (e)). Furthermore, supersaturated carbon atoms inside the Ni cluster gradually lift up the carbon-shell surface leading to a half-cap structure that appears after 40 ns (Fig. 2 (f)). This lifting-up of the carbon cap results in

formation of its stem, which can be regarded as an initial stage of the growth process of SWNT (Fig. 2 (g, f)).

3.2. Effect of vapor density

In this simulation, the density of carbon-source molecules gradually decreases by consumption as metal-carbon clusters. A typical density around 30 ns in Fig. 2 is about 150 molecules in a cubic cell of 20 nm. The number density of ideal gas molecules, $\rho = p/(k_\mathrm{B}T)$, at 10 Torr at 800 °C in real CVD experimental condition [6] is roughly 7 molecules in a cube of 20 nm. Hence, the density of the simulation is roughly 20 times higher, though it is quite difficult to compare it with actual experimental conditions.

In the next stage, where almost all the carbon atoms are absorbed to the catalytic metal particle and therefore no carbon-source molecules are left after 100 ns simulation, we pick up the Ni_{108} particle attached to the carbon cap at 100 ns and put it again into randomly allocated carbon-source molecules for next calculation. We test two cases, where the numbers of added carbon atoms are 150 and 500. The density of carbon vapor in the former case is optimum for the further growth of the cap structure in previous simulation (150 molecules per $(20\ \mathrm{nm})^3$), while that in the latter case is excessively higher.

Figure 3 shows snapshots after 50 ns calculation. The cap structure continues to grow in the optimum condition (Fig. 3 (a)), while in the non-optimum case incoming carbon atoms overwhelm an appropriate rate of tube growth and, as a result, the surface of the metal particle is coated with carbon atoms (Fig. 3(b)). This density of the carbon source is much higher than that in actual experiments, but we can qualitatively summarize that an optimum rate exists for the nucleation of the cap structure and the rate of carbon supply overwhelms that of the annealing process to a hexagonal network resulting in the overcoat of amorphous carbons.

3.3. Effect of metal cluster size

Figure 4 shows the snapshots of 100 ns calculation with Ni_{32} and Ni_{256} at 2500 K. In both conditions, the initial growth process is equal to that described above, that is, the absorbance of carbon atoms into the metal cluster until saturation followed by the formation of a hexagonal network and its lift-up. Starting from Ni_{32}, the whole surface of Ni_{32} is covered with the graphitic structure, and therefore the growth of the cap structure is terminated due to lack of further carbon supply from the surface (Fig. 4 (a)). On the other hand, in the case of Ni_{256}, (Fig. 4 (b)) an open metal surface is preserved and growth of the cap structure occurs at the surface of the cluster. In this case, the diameter of the cap is determined by the 'metal humps' working as a template of about 1.4 nm, which is smaller than that of the metal-carbon binary cluster. Here, the 'metal humps' looks like the grain boundary of metal crystal structure. Hence, the cap diameter of an SWNT is not necessarily equal to the diameter of catalytic metal in case it has suitable humps. Figure 4(c) shows the cross sectional view of the metal-carbon cluster from Ni_{256} at 20 ns. Embedded in the hexagonal carbon networks, nickel atoms are regularly allocated as observed experimentally [15]. Figure 4(c) implies a strong interaction between the graphite lattice and nickel atoms, which may be the key to the formation of the nanotube structure. The graphitic sheet extending between metal surfaces in Fig. 4(c) is the protrusion of the sheet from the 'metal hump'.

3.4. Summary

From these molecular dynamics simulations, the growth mechanism of SWNTs in CCVD may be summarized as follows. Carbon atoms are first absorbed into the metal cluster until saturation to make a hexagonal network of carbons inside the surface of the cluster. Further supply of carbon atoms leads to a separation of the carbon network from the metal surface itself or from a hump on the surface of the metal cluster, which in the end results in carbon cap formation. For further growth of the cap structure into an SWNT, some exposed areas must be retained on the cluster surface. If the catalytic metal cluster is a perfect sphere, the diameter of the cap may be correlated to that of the metal catalyst. However, the shapes of

the catalyst particles used in actual experiments are not ideally spherical; therefore the cap diameter does not necessarily correspond to that of the catalytic metal, especially if it has humps of suitable sizes. In general, lift-up of the cap structure is observed only when the cap diameter is reasonably large. Too small caps cannot be lifted because the curvature energy is too high. Another important observation is that the cap structure of a reasonable size is not directly formed as the lift-up of graphitic coating on the metal surface. They are always supplied initially from the hump as an open graphitic structure, probably because the lifting of coated graphitic structure needs high enough extra energy for cutting all metal-carbon bonds.

It may further be deduced that the crystal orientation may play a critical factor for the determination of chirality because our calculation indicates strong interaction between the hexagonal carbon network and the structure of catalytic metal atoms. Further understanding of the detailed function of metal catalyst is essential to achieve full control of the diameter and the chirality of SWNTs.

References

[1]   S. Iijima, T. Ichihashi, Nature 363 (1993) 603.

[2]   A. Thess, R. Lee, P. Nikolaev, H. Dai, P. Petit, J. Robert, C. Xu, Y.H. Lee, S.G. Kim, A. G. Rinzler, D. T. Colbert, G. E. Scuseria, D. Tománek, J. E. Fischer, R. E. Smalley, Science 273 (1996) 483.

[3]   C. Journet, W.K. Maser, P. Bernier, A. Loiseau, M.L. de la Chapelle, S. Lefrant, P. Deniard, R. Lee, J. E. Fisher, Nature 388 (1997) 756.

[4]   H. Dai, A.G. Rinzler, P. Nikolaev, A. Thess, D.T. Colbert, R.E. Smalley, Chem. Phys. Lett. 260 (1996) 471.

[5]   A.M. Cassell, J.A. Raymakers, J. Kong, H. Dai, J. Phys. Chem. B 103 (1999) 6484.

[6]   S. Maruyama, R. Kojima, Y. Miyauchi, S. Chiashi, M. Kohno, Chem. Phys. Lett. 360 (2002) 229.

[7]   M.J. Bronikowski, P.A. Willis, D.T. Colbert, K.A. Smith, R.E. Smalley, J. Vac. Sci. Technol. A 19 (2001) 1800.

[8]   M. Yudasaka, R. Yamada, N. Sensui, T. Wilkins, T. Ichihashi, S. Iijima, J. Phys. Chem. B 103 (1999) 6224.

[9]   H. Kataura, Y. Kumazawa, Y. Maniwa, Y. Ohtsuka, R. Sen, S. Suzuki, Y. Achiba, Carbon 38 (2000) 1691.

[10]   A. Maiti, C.J. Brabec, C. Roland, J. Bernholc, Phys. Rev. B 52 (1995) 14850.

[11]   A. Maiti, C.J. Brabec, J. Bernholc, Phys. Rev. B 55 (1997) 6097.

[12]   D.W. Brenner, Phys. Rev. B 42 (1990) 9458.

[13]   T. Kawai, Y. Miyamoto, O. Sugino, Y. Koga, Phys. Rev. B 66 (2002) 033404.

[14]   J. Gavillet, A. Loiseau, C. Journet, F. Willaime, F. Ducastelle, J.-C. Charlier, Phys. Rev. Lett. 87 (2001) 275504.

[15]   A.N. Andriotis, M. Menon, G. Froudakis, Phys. Rev. Lett. 85 (2000) 3193.

[16]   Y.H. Lee, S.G. Kim, D. Tománek, Phys. Rev. Lett. 78 (1997) 2393.

[17]   F. Banhart, J.-C Charlier, P.M. Ajayan, Phys. Rev. Lett. 84 (2000) 686.

[18] Y. Yamaguchi, S. Maruyama, Euro. Phys. J. D 9 (1999) 385.

[19] Y. Shibuta, S. Maruyama, Physica B 323 (2002) 187.

[20] S. Maruyama, Y. Shibuta, Mol. Cryst. Liq. Cryst. 387 (2002), 87.

[21] M. Kohno, S. Inoue, R. Kojima, S. Chiashi, S. Maruyama, Physica B 323 (2002) 272.

[22] Y. Yamaguchi, S. Maruyama, Chem. Phys. Lett. 286 (1998) 336.

[23] S. Maruyama, Y. Yamaguchi, Chem. Phys. Lett. 286 (1998) 343.

[24] H.J.C. Berendsen, J.P.M. Postma, W. F. van Gunsteren, A. DiNola, J. R. Haak, J. Chem, Phys. 81 (1984) 3684.

Figure Captions

Fig. 1 Initial condition of growth simulation for CCVD method. Completely random vapor mixture of 500 carbon-containing molecules and a nickel cluster are allocated in a 20 nm cubic periodic cell.

Fig. 2 Snapshots of the metal-catalyzed growth process of the cap structure: a 130 ns molecular dynamics calculation at 2500 K for Ni_{108}. Gray circles represent nickel atoms. Carbon atoms are not shown for clarity. Gray arrows show a typical supply route of carbon atoms from expose metal surface.

Fig. 3 Snapshots of a metal particle after 50 ns calculation with two density conditions. Gray circles represent nickel atoms. Carbon atoms are not shown for clarity.

Fig. 4 Snapshots of aggregation of carbon atoms on a nickel cluster of 100 ns: molecular dynamics calculations for (a) Ni_{32} and (b) Ni_{256}. A cross sectional view of the Ni_{256} cluster at 20 ns is shown in (c). Gray circles represent nickel atoms. Carbon atoms are not shown for clarity.
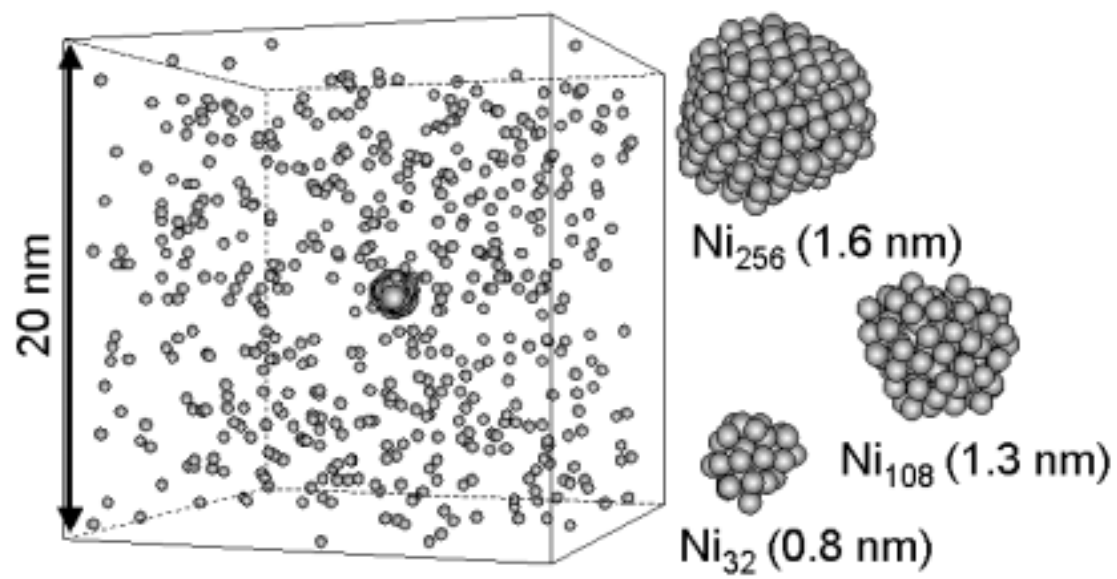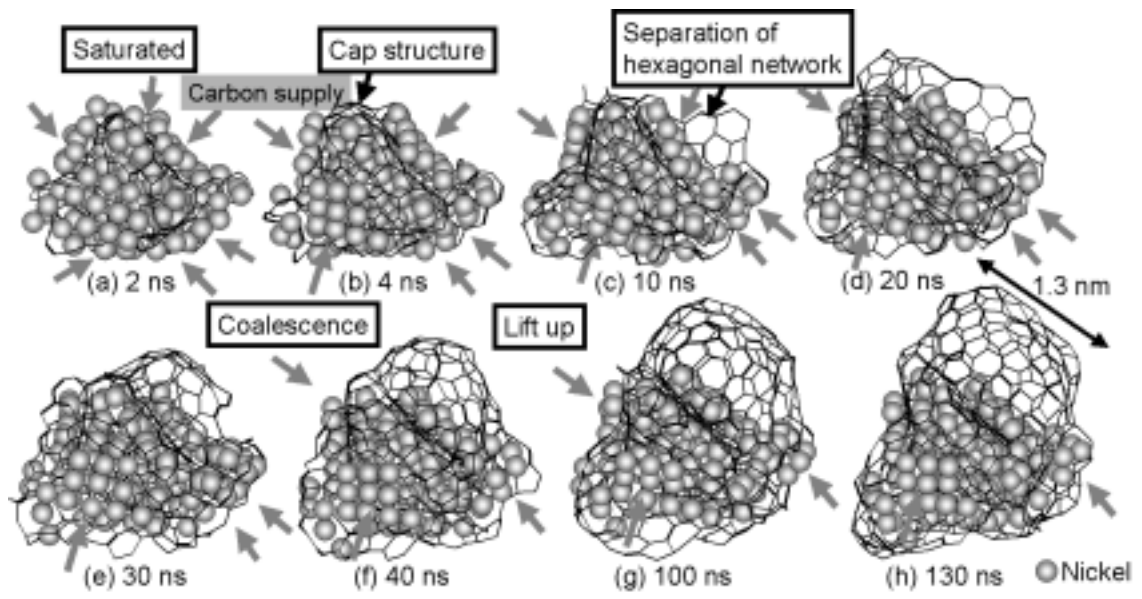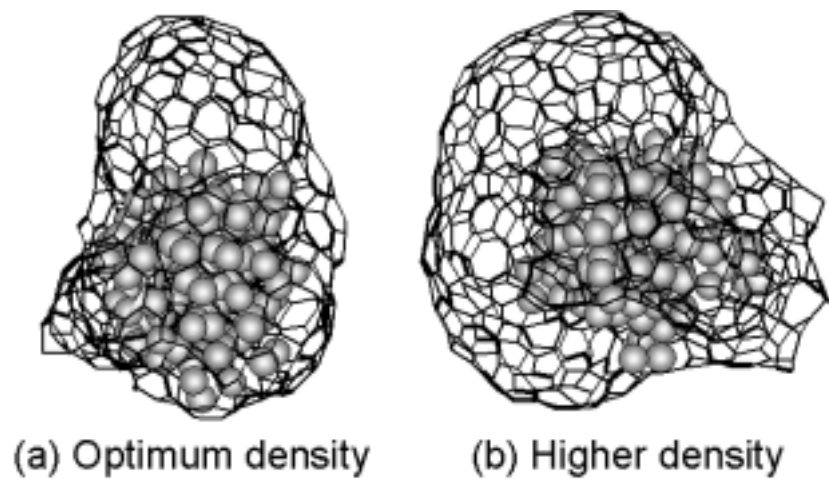
Ni$_{256}$ (1.6 nm)

Ni$_{108}$ (1.3 nm)

Ni$_{32}$ (0.8 nm)

Fig. 1

Fig. 2

(a) Optimum density   (b) Higher density

Fig. 3

(a) Ni$_{32}$
0 ns   20 ns   50 ns   100 ns

Carbon supply   ○ Nickel

(b) Ni$_{256}$
0 ns   20 ns   50 ns   100 ns

(c) Cross sectional view of Ni$_{256}$ at 20 ns   rotate

Slice view   rotate

Fig. 4